Short gravity waves due to a steadily-advancing ship hull

Francis Noblesse[1], Gerard Delhommeau[2], Fuxin Huang[3], Chi Yang[4]

[1] francis.noblesse@navy.mil; David Taylor Model Basin, NSWCCD, West Bethesda, MD, USA
[2] gerard.delhommeau@ec-nantes.fr; École Centrale de Nantes, CNRS, Nantes, France
[4] fhuang@gmu.edu; Dept of Computational and Data Sciences, George Mason University, Fairfax, VA, USA
[4] cyang@gmu.edu; Dept of Computational and Data Sciences, George Mason University, Fairfax, VA, USA

Introduction

We consider potential flow about a ship hull that advances at constant speed along a straight path in calm water, using a Green function that satisfies the radiation condition and the Kelvin-Michell linear free-surface boundary condition. This approach expresses the flow velocity $\widetilde{\mathbf{u}}(\widetilde{\mathbf{x}})$ generated by the ship hull at a flow field point $\widetilde{\mathbf{x}}$ as the sum of a local flow component and a wave component $\widetilde{\mathbf{u}}_W(\widetilde{\mathbf{x}})$ that is defined via a linear superposition of elementary water waves:

$$\left\{\begin{array}{c}\widetilde{u}_W\\ \widetilde{v}_W\\ \widetilde{w}_W\end{array}\right\} = \frac{1}{\pi F^2}\,\Im\mathrm{m}\int_{-\infty}^{\infty} dt\,\sqrt{1+t^2}\,e^{\,(1+t^2)\,\widetilde{z}\,/F^2+i\,\sqrt{1+t^2}\,(\widetilde{x}+t\,\widetilde{y})/F^2}\left\{\begin{array}{c}i\\ i\,t\\ \sqrt{1+t^2}\end{array}\right\}\widetilde{S}(t\,;\widetilde{x}) \tag{1}$$

The wave-spectrum function $\widetilde{S}(t\,;\widetilde{x})$ in this Fourier-Kochin representation of the wave component $\widetilde{\mathbf{u}}_W$ is given by a distribution of elementary water waves over the ship hull. E.g., if the flow is represented in terms of a distribution of sources, with density σ, over the surface H of the ship hull, we have

$$\widetilde{S}(t\,;\widetilde{x}) \equiv \frac{1}{F^2}\int_{H_e} da(\mathbf{x})\,e^{\,(1+t^2)\,z\,/F^2\,-\,i\,\sqrt{1+t^2}\,(\,x\,+\,t\,y\,)/F^2}\sigma(\mathbf{x}) \tag{2}$$

Here, H_e stands for the 'effective' portion of the hull surface H located ahead of the plane $x=\widetilde{x}$, in accordance with the step function $H(x-\widetilde{x})$ in the expression for the Green function, and above the horizontal plane $z=-7F^2/(1+t^2)$ because the exponential function in the integrand of (2) is smaller than 0.1% below this plane.

The X axis is taken along the path of the ship and points toward the ship bow, the Z axis is vertical and points upward, and the mean free surface is taken as the plane $Z=0$. The flow is observed from a moving system of Cartesian coordinates (X,Y,Z) attached to the ship and thus appears steady. The flow velocity in this moving frame of reference is given by $(U-V_s\,,V,W)$ where V_s stands for the ship speed and $\mathbf{U}\equiv(U,V,W)$ is the (disturbance) flow due to the ship. The coordinates of the flow-field point $\widetilde{\mathbf{x}}$ in (1) and the source point $\mathbf{x}$ in (2) are nondimensional in terms of the ship length L_s, and $F\equiv V_s/\sqrt{g\,L_s}$ is the Froude number.

The waterline integral in the Neumann-Kelvin theory of ship waves has a large effect

Before we consider short waves, we note that the classical Neumann-Kelvin theory of ship waves involves both a surface distribution of sources over the mean ship hull H, considered in (2), and a line distribution of sources around the mean ship waterline Γ. Specifically, the Neumann-Kelvin theory of ship waves expresses the flow velocity $\widetilde{\mathbf{u}}$ as

$$\widetilde{\mathbf{u}} = \int_H da\,\widetilde{\nabla}G\,\sigma - F^2\int_\Gamma d\ell\,\widetilde{\nabla}G\,\sigma\,(n^x)^2/\sqrt{(n^x)^2+(n^y)^2} \equiv \widetilde{\mathbf{u}}^H + \widetilde{\mathbf{u}}^\Gamma \tag{3}$$

where the unit vector $\mathbf{n}\equiv(n^x,n^y,n^z)$ is normal to the ship hull surface H and points into the water. The line distribution of sources around the waterline Γ has a large influence, as shown in Fig.1 for the particular case in which the source density σ in (3) is taken as $\sigma=n^x$ in accordance with the slender-ship approximation proposed in [1].

Specifically, Fig.1 shows wave profiles for the usual parabolic Wigley hull (with parabolic framelines) at six Froude numbers $F=0.25$, 0.267, 0.289, 0.316, 0.354, 0.408. The symbols in this figure correspond to experimental measurements performed at the University of Tokyo. The two theoretical wave profiles in Fig.1 correspond to the slender-ship approximation defined by (3), with $\sigma=n^x$, and the related approximation $\widetilde{\mathbf{u}}^H$ in which the waterline integral around Γ is ignored. Differences between these two slender-ship approximations are significant, even though the line integral is $O(n^x)^3$ and the hull-surface integral is $O(n^x)$. In particular, the slender-ship approximation $\widetilde{\mathbf{u}}^H+\widetilde{\mathbf{u}}^\Gamma$ is significantly less oscillatory than the related slender-ship approximation $\widetilde{\mathbf{u}}^H$. In this respect, the approximation $\widetilde{\mathbf{u}}^H+\widetilde{\mathbf{u}}^\Gamma$ is in better agreement with experimental measurements than the approximation $\widetilde{\mathbf{u}}^H$. However, the bow wave predicted by the approximation $\widetilde{\mathbf{u}}^H$ is significantly higher, and closer to experimental measurements, than the bow wave given by $\widetilde{\mathbf{u}}^H+\widetilde{\mathbf{u}}^\Gamma$. The large influence of the waterline integral in (3) is easily explained theoretically [1].

There is a practical need for filtering short gravity waves

The wavelength $\lambda\equiv 2\pi F^2/(1+t^2)$ of the elementary water waves in the Fourier integral (1) vanishes as $t\to\pm\infty$. Short gravity waves are not physically realistic because they are significantly affected by surface tension and viscosity, ignored in (1). Furthermore, short waves have little practical effect on main flow characteristics relevant to determine

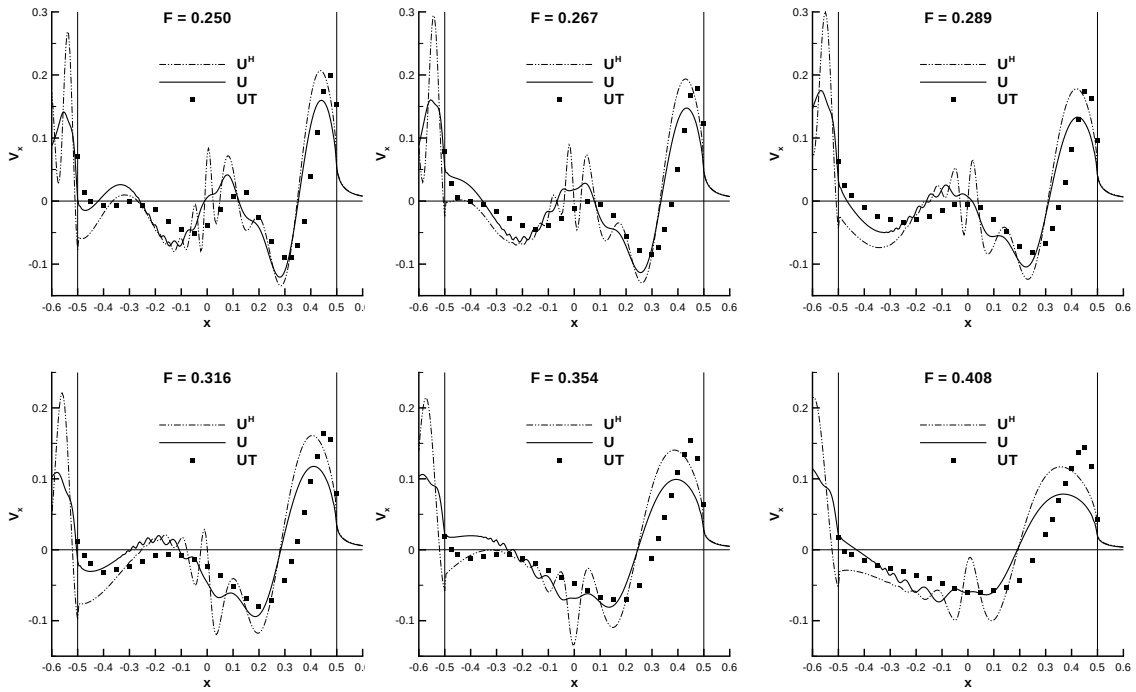

Figure 1: Wave profiles given by the slender-ship approximation (3), with $\sigma = n^x$, and the related slender-ship approximation $\widetilde{\mathbf{u}}^H$, in which the waterline integral around Γ is ignored, for the parabolic Wigley hull at six Froude numbers F. The symbols represent experimental measurements.

the wave profile along the ship waterline, the velocity and pressure distributions at the ship hull, and the related wave drag and hydrodynamic lift and moment. Lastly, a huge number of very small panels would be required to evaluate short waves within the framework of a low-order panel method. Indeed, the practical need for filtering unrealistic and troublesome short gravity waves is well understood, and the filtering of short waves is an important aspect of a numerical evaluation of the flow velocity defined by a flow representation that ignores viscosity and surface tension.

Short gravity waves can be filtered in a simple way

Waves with wavelengths λ shorter than some cutoff wavelength λ_∞ are then eliminated here. The choice of the cutoff wavelength λ_∞ is a matter of judgment, to some extent. An obvious choice is to take λ_∞ as a small fraction of the wavelength $2\pi F^2$ of the transverse waves generated by a ship advancing at a Froude number F. However, this choice is meaningful only at low Froude numbers. Indeed, at high Froude numbers, the wavelength $2\pi F^2$ is large in comparison to the transverse dimensions — notably the beam B and the draft D — of the ship hull, which largely determine the variation of the flow velocity. Thus, at high Froude numbers, it is reasonable to choose the cutoff wavelength λ_∞ as a small fraction of a (nondimensional) characteristic transverse dimension L^{BD}/L_s of the ship hull. The choice

$$L^{BD} \equiv BD/(B/2 + D)$$

yields $L^{BD} = R$ for a ship hull with circular cross section of radius R, $L^{BD} \approx D \approx B/2$ if $D \approx B/2$, $L^{BD} \approx 2D$ if $D \ll B$ and $L^{BD} \approx B$ if $B \ll D$. We also have $L^{BD} \leq B$ and $L^{BD} \leq 2D$. The ratio

$$\sigma^H \equiv \frac{L^{BD}}{L_s} \equiv \frac{b\,d}{b/2 + d} \quad \text{with} \quad b \equiv \frac{B}{L_s} \quad \text{and} \quad d \equiv \frac{D}{L_s} \tag{4}$$

is a nondimensional transverse ship dimension or 'hull-slenderness' parameter. For instance, we have $\sigma^H = 0.06$ for $b = 0.15$ and $d = 0.05$.

The cutoff wavelength λ_∞ is then taken as $\lambda_\infty = \varepsilon_0\, 2\pi F^2$ or $\lambda_\infty = \varepsilon_\infty\, \sigma^H$ as $F \to 0$ or $F \to \infty$, respectively. The relation $\lambda_\infty = 2\pi F^2/(1 + t_\infty^2)$ yields

$$t_\infty \approx \frac{1}{\sqrt{\varepsilon_0}} \text{ for } F \leq F_t \quad \text{and} \quad t_\infty \approx \frac{2.5}{\sqrt{\varepsilon_\infty}}\,\frac{F}{\sqrt{\sigma^H}} \text{ for } F_t \leq F \quad \text{with} \quad F_t \equiv 0.4\sqrt{\frac{\varepsilon_\infty}{\varepsilon_0}}\,\sqrt{\sigma^H} \tag{5}$$

Thus, t_∞ is proportional to F except at low Froude numbers $F < F_t$. For $\varepsilon_0 = 0.03$, we have $t_\infty \approx 5.8$ for $F \leq F_t$, with $F_t \approx 0.13$ for $\varepsilon_\infty = 0.05$ and $\sigma^H = 0.06$. These values of ε_∞ and σ^H also yield $t_\infty \approx 45.6\,F$ for $F_t \leq F$, i.e. $t_\infty \approx 45.6$, 22.8, 16, 11.4, 6.8 for $F = 1$, 0.5, 0.35, 0.25, 0.15.

Filtering of short waves is mostly required if $\widetilde{z} < 0$. Indeed, the exponential function $\widetilde{E} \equiv e^{(1+t^2)\,\widetilde{z}/F^2}$ vanishes (rapidly) as $t \to \infty$ if $\widetilde{z} < 0$, but $\widetilde{E} = 1$ for all values of t if $\widetilde{z} = 0$. Convergence of the Fourier integral (1) therefore is significantly slower for $\widetilde{z} = 0$ than for $\widetilde{z} < 0$. The function $\widetilde{E}$ is then multiplied by a function Λ that vanishes as $t \to \infty$; e.g.,

$$\Lambda \equiv e^{-5\,|t|^N/t_\infty^N}\,. \tag{6a}$$

The function (6a) differs from 1 by less than 1% for $0 \le |t| \le t_* \equiv \sigma_* t_\infty$ with $\sigma_* \approx 0.3$, 0.5, 0.7, 0.9 for $N = 5$, 9, 17, 59. The Fourier representation (1) of the velocity components $\widetilde{u}_W$, $\widetilde{v}_W$ and $\widetilde{w}_W$ involve the factors i, $i\,t$ or $\sqrt{1+t^2}$, respectively. The functions t and $\sqrt{1+t^2}$ evidently increase like t as $t \to \infty$. Thus, convergence of the Fourier integral (1) is significantly slower for the components $\widetilde{v}_W$ and $\widetilde{w}_W$ than for the component $\widetilde{u}_W$. It is then convenient to replace t in the factors $i\,t$ or $\sqrt{1+t^2}$ associated with the velocity components $\widetilde{v}_W$ and $\widetilde{w}_W$ by $t\theta$ with the function θ defined as

$$\theta = (1+100\,|t|^{M-1}/t_\infty^M)/(\,1+100\,|t|^M/t_\infty^M\,)\,. \tag{6b}$$

We have $t\theta \sim t$ as $t \to 0$, $t\theta \sim 1$ as $t \to \infty$, and $t\theta = t_\infty \theta_\infty \equiv (t_\infty + 100)/101$ for $t = t_\infty$. We then have $1 \le t_\infty \theta_\infty < 1.2$ for $1 \le t_\infty < 20$. The function (6b) differs from 1 by less than 1% for $0 \le |t| \le t_* \equiv \sigma_* t_\infty$ with $\sigma_* \approx 0.3$, 0.5, 0.7, 0.9 for $M = 8$, 13, 25, 87. The approximations $\Lambda \approx 1$ and $\theta \approx 1$ for $0 \le |t| \le t_*$ mean that no appreciable wave damping occurs within the range $0 \le |t| \le t_*$ and that filtering mostly occurs within the range $t_* < |t| \le t_\infty$. This wave-damping range represents 10% of the integration range $0 \le |t| \le t_\infty$ for $\sigma_* = 0.9$, which thus corresponds to a fairly fast and computationally efficient filter. However, for $\sigma_* = 0.5$, the wave-damping range represents 50% of the integration range, which means a slower and less efficient filter. The moderately efficient filter $\sigma_* = 0.7$, i.e. $N = 17$ and $M = 25$, is a reasonable compromise. Thus, the Fourier representation (1) is modified as

$$\left\{\begin{array}{c} \widetilde{u}_W \\ \widetilde{v}_W \\ \widetilde{w}_W \end{array}\right\} = \frac{1}{\pi F^2}\,\Im\mathrm{m}\int_{-t_\infty}^{t_\infty} dt\,\Lambda\,\sqrt{1+t^2}\,e^{(1+t^2)\,\widetilde{z}/F^2 + i\,\sqrt{1+t^2}\,(\widetilde{x}\,+\,t\,\widetilde{y})/F^2} \left\{\begin{array}{c} i \\ i\,t\,\theta \\ \sqrt{1+t^2\theta^2} \end{array}\right\} \widetilde{S}(t\,;\widetilde{x}) \tag{6c}$$

where Λ and θ are given by (6a) with $N = 17$ and (6b) with $M = 25$.

Calculations, for a modified Wigley hull that has triangular (instead of parabolic) framelines, of the wave component $\widetilde{\mathbf{u}}_W$ defined by (1) and (2) with the source density σ taken as $\sigma = n^x$, show that both the functions Λ and θ have significant effects, and that large values of the parameters N and M are preferable. When used in addition to the filter Λ, the filter θ only has a relatively small beneficial effect on $\widetilde{v}$ and $\widetilde{w}$, as expected because the function Λ already filters short waves. The two filters Λ and θ can then be used together, e.g. with the consistent values $N = 17$ and $M = 25$ that both correspond to $\sigma_* \approx 0.7$. Calculations show that $N = 17$ and $M = 25$ indeed are reasonable choices, and that the choices $\varepsilon_\infty = 0.05$ and $\varepsilon_0 = 0.03$ in expressions (5) for the upper limit of integration t_∞ are reasonable.

The left, center and right columns in Fig.2 show the wave components $\widetilde{u}_W$, $\widetilde{v}_W$ and $\widetilde{w}_W$, respectively, given by (5) with $N = 17$, $M = 25$ and (2) with $\sigma = n^x$ for a modified Wigley hull (with triangular framelines) at five Froude numbers $F = 0.15$ (top row), 0.25, 0.35, 0.5 and 1 (bottom row). The low-speed filtering parameter ε_0 in (5) is chosen as $\varepsilon_0 = 0.03$ for the calculations reported in Fig.1, where three values $\varepsilon_\infty = 0.01$, 0.05, 0.1 of the high-speed filtering parameter ε_∞ are considered. For the modified Wigley hull considered here, for which we have $b = 1/10$, $d = 1/16$ and $\sigma^H = 1/18$, the transition Froude number F_t defined by (5) is approximately equal to 0.05, 0.12, 0.17 for $\varepsilon_\infty = 0.01$, 0.05, 0.1 and $\varepsilon_0 = 0.03$. These Froude numbers are below the range $0.15 \le F \le 1$ considered in Fig.2, except in one case that corresponds to $F = 0.15$ and $\varepsilon_\infty = 0.1$. The choices $\varepsilon_\infty = 0.01$, 0.05, 0.1 yield velocities $\widetilde{u}_W$, $\widetilde{v}_W$, $\widetilde{w}_W$ that are not very different. A relatively large value of ε_∞ can then be chosen, a choice that lowers the upper limit of integration t_∞ defined by (5) and therefore reduces computational efforts. Fig.2 also shows that differences are more important for smaller Froude numbers, for which short gravity waves appear to have relatively more notable effects. The transverse components $\widetilde{v}_W$ and (especially) $\widetilde{w}_W$ of the flow velocity $\widetilde{\mathbf{u}}_W$ in Fig.2 are appreciably larger than the longitudinal component $\widetilde{u}_W$, in accordance with the theory of flow about a slender body in translatory motion.

Conclusion

The short-wave filter defined by (6) with (5) and (4) is defined explicitly, and a priori, in terms of the speed and the major dimensions (length, beam and draft) of a ship. The classical Neumann-Kelvin theory of ship waves involves a line integral around the ship waterline that has a large influence. Further details may be found in [2], where a practical mathematical representation of the flow representation (3) is given.

References

[1] Noblesse F (1983) A slender-ship theory of wave resistance, J. Ship Research, 27:13-33

[2] Noblesse F, Delhommeau G, Huang F, Yang C (submitted) Practical mathematical representation of the flow due to a distribution of sources on a steadily-advancing ship hull

Acknowledgments

This work was sponsored by the Office of Naval Research; Ms. Kelly Cooper is the Technical Monitor.

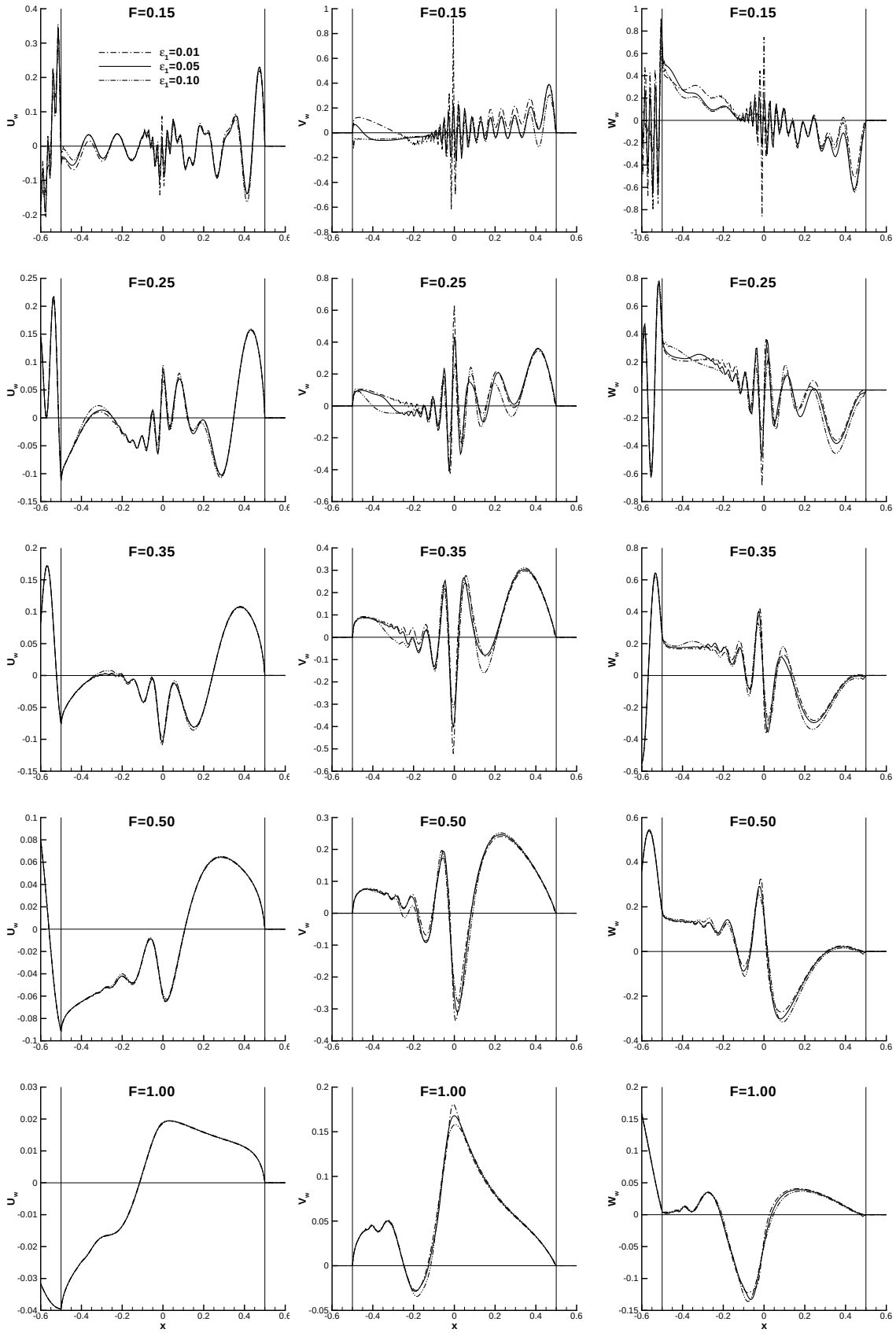

Figure 2: Wave components $\widetilde{u}_W$ (left), $\widetilde{v}_W$ (center), $\widetilde{w}_W$ (right) given by (5) with $N = 17$, $M = 25$ and (2) with $\sigma = n^x$ for a modified Wigley hull at $F = 0.15$ (top), 0.25, 0.35, 0.5, 1 (bottom). The three curves correspond to $\varepsilon_\infty = 0.01$, 0.05, 0.1 with $\varepsilon_0 = 0.03$.